Double Stratification Phenomenon on Stagnation Point Flow of a Micropolar Nanofluid over a Porous Medium with Activation Energy and Chemical Reaction

Meena Rajeswari P and *Poulomi De

Department of Mathematics, School of Advanced Sciences, Vellore Institute of Technology,

Chennai-600127, Tamilnadu, India.

Corresponding Author-*P.De, Email: poulomi.de@vit.ac.in; Tel. /Fax: +91 44 3993 1555, Ph. No. +91 94448 84134 and P. Meena Rajeswari, Email: meenuraji1799@gmail.com

Abstract

This study explored the double-stratified micropolar nanofluid stagnation point flow enclosed by porous medium with activation energy and chemical reaction. The phenomena of hydrodynamic magnetic field acting normal direction to stretching surface also incorporated here. System of governing equations are owned by key parameters and converted into ordinary differential equations (ODE's) with help of similarity transformation. Numerical solutions are encountered with the aid of Runge-Kutta-Fehlberg 5^{th} order method, accompanied by shooting technique. Comparison between skin friction coefficient and local couple stress in micropolar constant and porous parameter with well-known research findings is also reported. Numerical formulation and investigation are made on local skin friction, local couple stress, heat and mass transfer rate in various parameters. A pictorial representation of abundant parameters on linear and angular velocity, temperature and concentration field is analysed. The gradual gain of the micropolar constant enhances the fluid's velocity and angular velocity profile. Solutal and chemical reaction rate constant are diminish the mass transfer of fluid. This study can be used in many eye-catching applications, such as biomedical engineering, lap-on-a-chip devices, cooling agent in electrical devices, automobiles and oil recovery processes.

Keyword: Micropolar nanofluid; Stagnation point; Stratification; Porous medium; Activation energy; Chemical reaction

1. Introduction

Micropolar fluid plays an important role and is a highly viewed topic in current research due to its microstructure property. It enhances the heat transfer property of fluids. Micropolar fluid is useful in variety of fields, such as biomedical engineering, micro-fluidics, oil recovery processes, cooling agents for electrical components, heat exchangers and material refining. Non-Newtonian fluid type of micropolar fluid, which has micro-rotation and micro-inertia property and pursues both linear and angular motion of fluid flow, for achieving high results we have to add upon nanoparticles in this study, so micropolar nanofluid has more efficient power in many applications. Micropolar nanofluids have a microstructure that is utilized in biomedical field for effective drug-conducting systems within the body and their small-scale behaviours are

used in chip devices, chemical analysis zones and micro-fluidic devices. Micropolar nanofluid acts as a cooling agent in electrical devices; it can reduce the resistance of heat transfer, so excessive thermal energy evaporation should be cut off in vehicle engines, electrical devices and power systems. So micropolar nanofluid gives efficient cooling power in vehicle motors and batteries. This notable micropolar nanofluid was highlighted by Eringen [1, 2] and he developed its usages. Hsiao [3] studied the heat and mass transfer of magnetohydrodynamic micropolar fluid flow. This motion involved a spin vector towards stretching sheet to investigate viscous dissipation effects in multimedia features and they used an accurate finite difference method for solving differential equations. Eldabe and Ouaf [4] presented heat and mass transfer of MHD micropolar fluid flow with Ohmic heating and viscous dissipation effects along the stretching surface and Chebyshev finite difference method was used to earn numerical solution. Mishra et al. [5] include the shrinking sheet surface for free convective micropolar fluid's heat transfer with heat source and the Runge-Kutta method used for solving ordinary differential equations (ODE's).

In fluid flow, a point with zero velocity that is called stagnation point, the fluid flow in the vicinity of stagnation point is refers stagnation point flow. When we include this topic in micropolar nanofluid, it helps to improve design of cooling systems and make poor drag for improve good fluid flow. Hsiao [6] studied the mixed convection of stagnation electromagnetohydrodynamic (EMHD) nanofluid on the stretching sheet and the equation is derived by similarity transformation technology. Soid et al. [7] reviewed the stagnation point flow of a micropolar fluid over a stretching and shrinking sheet, including the slip boundary conditions and Matlab boundary value problem solver used to get solved equations. Muhammad et al. [8] analyzed the EMHD and stagnation point flow of micropolar fluid in the presence of nanoparticles and the inclusion of mixed convection and slip boundary. Here, the shooting technique is used. Hsiao [9] explored heat transfer analysis on Maxwell fluid with radiative and viscous dissipation effects with EMHD effect, solving equations by the way of finite difference method. Gamar et al. [10] discovered the stagnation magnetohydrodynamic (MHD) micropolar nanofluid flow with thermal radiation and Navier slip via stretching sheet with Runge-Kutta-Fehlberg (RKF) method.

When fluid flow passes through temperature difference and concentration difference, it creates different layers in fluid structure. This phenomena is called thermal stratification and solutal stratification respectively. Atif et al. [11] investigate the flow of MHD stratified micropolar nanofluid in the presence of gyrotactic microorganisms with thermal radiation and Joule heating collaboration and numerical solution tackled by the shooting method. Sarojamma et al. [12] explored the effects of thermal and solutal stratification on double diffusive convective micropolar fluid flow and investigated the heat and mass transfer of fluid flow. The ODE's were solved by RKF-45 algorithm with shooting technique. Alharbi et al. [13] ascertained the development in heat transfer due to EMHD bioconvective flow of micropolar nanofluid flow with thermal radiation effect and stratification through a stretching sheet and non-linear differential system solved by bvp4c algorithm. Farooq et al. [14] verified the combined effect of melting heat transfer and double stratification in viscous nanofluid flow at stagnation point and obtained numerical solutions via shooting method. Choudhary et al. [15] discovered the nature of tangent hyperbolic fluid with double stratification, stagnation and dual convection flow induced by stretching cylinders and bvp5c exactness program used to obtain numerical solutions.

Porous medium looks like a sponge structure; it has a lot of void space. The amount of fluid flow is recognised by its permeability of pore size. Abbas Khan et al. [16] ascertained the micropolar nanofluid flow via porous exponential stretching sheet and numerically solved by MATLAB bvp4c. Mohanty et al. [17] used the Runge-Kutta (RK) 4^{th} order method with shooting technique to numerically investigate the heat and mass

flow of micropolar fluid on a stretching sheet in the medium of porous structure. Dadheech et al. [18] studied Oldroyd-B fluid flow through porous medium in the presence of melting, chemical and slip effects and equations are resolved by bvp4c inbuilt MATLAB. Karthik et al. [19] analysed Cattaneo-Christow Powell Eyring fluid model of MHD fluid with heat sink, chemical reaction and porous medium and MATLAB's BVP4C solver method employed. De [20] explored the nanofluid flow with Ohmic heating and bioconvection effects saturated in porous medium and ODE dissolved by the 5^{th} order Runge-Kutta-Fehlberg method and shooting technique. Goyal et al. [21] analysed the effect of heat absorption/generation and melting phenomena on micropolar fluid flow derived by RK 4^{th} order method. Mishra et al. [22] studied the viscous fluid flow in stagnation point inclusion of non-Darcy porous medium and heat source/sink over a stretching sheet used the RK 4^{th} order method for solving purpose.

Chemical reactions are included for enhance fluid flow operations, but sometime they can lead to some burden on flow, that's why we need activation energy. Activation energy boosts the molecules. Fluid microparticle requires minimum energy to react with chemicals, so activation energy provided that. Nisha and De [23] used RKF 5^{th} order method to explore the impact of electro-osmotic, activation energy and chemical reaction on Sisko fluid through stretching cylinder in the presence of Darcy-Forchheimer porous medium. Senbagaraja and De [24] presented EMHD tangent hyperbolic nanofluid flow via porous rotating disk with the effects of chemical reaction, variable thermal conductivity and Stefan blowing by usage of RKF 5^{th} order method. Yesodha et al. [25] studied activation energy along with soret and dufour effects in chemically reacting fluids, which also included heat and transfer property analysis in the porous stretched sheet. Prakash et al. [26] investigate the transient convective heating transport phenomena in micropolar fluid flow with activation energy between the asymmetric surface and Crank-Nicolson implicit finite difference method is adapted to find numerical solution. Zeeshan et al. [27] presented built-in algorithm for numerical intuition and explored the activation energy and thermal radiation effects in transient micropolar nanofluid flow on a plat surface. Hsiao [28] analysed the efficiency of Carreau-nanofluid flow in the presence of activation energy, EMHD with parameters control method and equations are resolved by implicit finite difference method. Lakshmi et al. [29] classify the effects of chemical reactions, radiation and activation energy on magnetohydrodynamic nanofluid flow induced by buoyancy effects past a vertical surface. Soliman [30] studied about temperature dependent heat generation on MHD micropolar nanofluid flow with variable porous matrix structure and transformed ODE's cleared by shooting techniques. Vinodkumar reddy et al. [31] discussed about Casson nanofluid flow embedded in porous medium with MHD and activation energy in the presence of suction and injection and numerically solved via the bvp5c MATLAB. Raza et al. [32] analysed the thermal conductivity over Darcy forchheimer double porous medium in bio convective nanoparticles flow with chemical reaction and activation energy also includes the ternary hybrid ferrofluid in heat transfer process. Gomari et al. [33] discovered the forced convection of heat in stagnation nanofluid flow over porous media and analyse the entropy generation in cylinder. Vijayaragavan et al. [34] studied the peristaltic motion of fluid influenced by chemical reaction, magnetic field and porous medium and computational analysis done by Matlab.

The current trends laminar flow concept collaborated with accelerated flow on ψ-v scheme of the Navier-Stokes equations analysed through various geometry such as vortex dynamics and compact nonuniform grids taken by Kumar and Kalita [35-37]. Khan et al. [38] studied the compressible flow by convolutional neural network model, this articles also adds advanced flow study about laminar nanofluid flow.

1.1. Objective and Applications of Present Study

The above literature review gives clear navigation for this current study which is stated as follows:

i. Mainly micropolar fluid taken due to its micro-rotation property, it can expand the uses of current results in many applications such developing electrical device cooling systems to reduce excessive heat generation and make cost-effective, compatibility and stability based electric devices, engines and power systems.

ii. Inclusion of Stratification phenomenon is significant to enhance the fluid flow configuration.

iii. The structure of micropolar nanofluid flows in porous medium replicates the blood flow in body tissues, so this study can improve the design of drug delivery systems in biomedical field and can properly conduct medicine and drugs within the body.

iv. Incorporate the activation energy and chemical reaction enhances the efficiency of nanoparticles, also their movements are examined by thermophoresis and Brownian motion effects. This study can help to understand fluid dynamic in various real-life applications.

1.2. Research Gap and Novelty

Brief study about literature survey demonstrated in Table 1. From this we can clearly address the research gap; generally the authors focused on developing micropolar fluid flow on simple configuration. When we analyse about stagnation micropolar nanofluid flow with double stratification effects through porous stretching sheet in the presence of activation energy and chemical reaction adds more advancement in applications. This non-Newtonian fluid model replicates real time scenario as obstacle in fluid motion, then how nanoparticles enhance the flow behaviour. Here we conduct this by adding stagnation point in micro-rotation fluid and by analysing nanoparticles clustering by Brownian motion and thermophoresis effects. Additionally stratification effects analyse the fluid's layer formation due to temperature and concentration difference in porous medium. Activation and chemical reaction enrich the overall performance of current result. Numerical results are done by Runge-Kutta-Fehlberg 5th order method along with shooting technique.

2. **Theory Formulation**

A two dimensional incompressible study micropolar nanofluid flow has been taken here for this study. This micro-rotational flow cooperated with stagnation point flow immersed with porous medium for better result thermal and solutal stratification is also induced. Activation energy and chemical reaction have also been considered with the aim of improving the result. The above phenomena were taken in the stretching sheet with stretching velocity $U_w = bx$ in the restricted flow region of $y > 0$. Consider stretching surface along x axis and fluid flow towards the x direction. A magnetic field $B(x) = B_0$ is acts perpendicular to the stretching sheet (refer Fig.1). All the above constraints made on Fig. 1 and governing equations are construct with it and given below (Hsiao [3]).

$$\frac{\partial u}{\partial x} + \frac{\partial v}{\partial y} = 0, \tag{1}$$

$$u\frac{\partial u}{\partial x} + v\frac{\partial u}{\partial y} = \left(\nu + \frac{k_f}{\rho}\right)\frac{\partial^2 u}{\partial y^2} + \frac{k_f}{\rho}\frac{\partial N^*}{\partial y} + U_e\frac{dU_e}{dx} - \left(\frac{\sigma B_0^2}{\rho} + \frac{\nu}{k_1}\right)\left(u - U_e\right), \tag{2}$$

$$u\frac{\partial N^*}{\partial x} + v\frac{\partial N^*}{\partial y} = \frac{\gamma}{j\rho}\frac{\partial^2 N^*}{\partial y^2} - \frac{k_f}{j\rho}\left(2N^* + \frac{\partial u}{\partial y}\right), \tag{3}$$

$$u\frac{\partial T}{\partial x}+v\frac{\partial T}{\partial y}=\alpha\frac{\partial^2 T}{\partial y^2}+\tau\left(D_B\frac{\partial C}{\partial y}\frac{\partial T}{\partial y}+\frac{D_T}{T_\infty}\left(\frac{\partial T}{\partial y}\right)^2\right), \tag{4}$$

$$u\frac{\partial C}{\partial x}+v\frac{\partial C}{\partial y}=D_B\frac{\partial^2 C}{\partial y^2}+\frac{D_T}{T_\infty}\frac{\partial^2 T}{\partial y^2}-K_r^2\left(C-C_\infty\right)\left(\frac{T}{T_\infty}\right)^m\exp\left(\frac{-E_a}{TK_1}\right). \tag{5}$$

Respective boundary conditions are (Soid et al. [7] & Atif et al. [11]),

$$u=U_w=bx,\ v=0,\ N^*=0,\ T=T_w=T_0+a_1x,\ C=C_w=C_0+d_1x \text{ at } y=0,$$

$$u=U_e=ex,\ N^*=0,\ T=T_\infty=T_0+a_2x,\ C=C_\infty=C_0+d_2x \text{ as } y\to\infty. \tag{6}$$

From the above equation, The velocity components u and v passes through x and y directions respectively, U_e represents the free stream velocity, B_0 denotes the magnetic field intensity, kinematic viscosity denote as ν, k_f be the vortex viscosity, ρ refers the density of the fluid, σ represents the fluid electric conductivity, k_1 be the permeability constant of porous medium, T and C denotes the temperature and concentration of the fluid, N^* denotes the dimensionless components of microrotation or angular velocity, thermal diffusivity of fluid denote as α, τ be the ratio of nanoparticles capacity of heat and base fluid , D_B is the Brownian diffusion coefficient, D_T be the thermophoresis diffusion coefficient, C_∞ and T_∞ refers the ambient fluid concentration and temperature, K_r be the chemical reaction constant, E_a is the activation energy, K_1 denotes Boltzmann constant and m as fitted rate.

Let us assume, the spin gradient viscosity γ in (3), is

$\gamma=\left(\mu+\frac{k_f}{2}\right)j$, where $j=\frac{\nu}{b}$ be the micro inertia density.

By the use of following similarity transformation: (Atif et al. [11]),

$$\left.\begin{aligned}&\eta=\sqrt{\frac{b}{\nu}}y,u=bxf'(\eta),v=-\sqrt{b\nu}f(\eta),N^*=\sqrt{\frac{b^3}{\nu}}xg(\eta),\theta(\eta)=\frac{T-T_\infty}{T_w-T_0},\\&\phi(\eta)=\frac{C-C_\infty}{C_w-C_0}\end{aligned}\right\} \tag{7}$$

Substituting Equation 7 into Equation 1-6, then we get transformed system of ordinary differential equations as Equation 8-11 and corresponding boundary conditions (Equation 12) also its satisfies the continuity equation (1) and remaining are

$$(1+K)f'''+ff''-f'^2+Kg'+A^2-\left(f'-A\right)\left(Ha+K^*\right)=0 \tag{8}$$

$$\left(1+\frac{K}{2}\right)g''-gf'+fg'-K\left(2g+f''\right)=0 \tag{9}$$

$$\theta''+\Pr\left(f\theta'-f'\theta-S_1f'+Nb\phi'\theta'+Nt\theta'^2\right)=0 \tag{10}$$

$$\phi''+\Pr Le\left(f\phi'-f'\phi-S_2f'\right)+\frac{Nt}{Nb}\theta''-\varepsilon\Pr Le\phi\left(1+\theta\delta\right)^m\exp\left(\frac{-E^*}{1+\theta\delta}\right)=0 \tag{11}$$

Corresponding boundary conditions,

$$f=0,\ f'=1,\ g=0,\ \theta=1-S_1,\ \phi=1-S_2,\ \text{at}\ \ \eta=0.$$

$$f'\to A,\ g\to 0,\ \theta\to 0,\ \phi\to 0,\qquad \text{at}\ \eta\to\infty. \tag{12}$$

Here, $K=\frac{k_f}{\mu}$ shows the micropolar constant, $A=\frac{e}{b}$ refers the ratio of stretching rate constant, $Ha=\frac{\sigma B_0^2}{\rho b}$ be the Hartmann number, $K^*=\frac{\nu}{k_1b}$ represents the porous parameter, Prandtl number notated as $\Pr=\frac{\nu}{\alpha}$, thermal and solutal stratification parameters are denoted as $S_1=\frac{a_2}{a_1}$ and $S_2=\frac{d_2}{d_1}$, $Nb=\frac{D_B}{\nu}\tau\left(C_w-C_0\right)$ shows the Brownian motion parameter, $Nt=\frac{D_T\tau}{T_\infty\nu}\left(T_w-T_0\right)$ denotes the thermophoresis parameter, Lewis number notated as $Le=\frac{\alpha}{D_B}$, $\varepsilon=\frac{K_r^2}{b}$ be the chemical reaction rate constant, $\delta=\frac{T_w-T_0}{T_\infty}$ shows the temperature ratio and $E^*=\frac{E_a}{K_1T_\infty}$ is the parameter of Activation energy.

Physical quantities of skin friction coefficient, the local couple stress, the Nusselt number and the Sherwood number are defined as (Hsiao [3])

$Cf_x=\frac{\tau_w}{\rho U_w^2}$ where $\tau_w=\mu\left[\left(1+K\right)\frac{\partial u}{\partial y}\right]_{y=0}$ is the shear stress,

$M_x=\frac{M_w}{\rho xU_w^2}$ here $M_w=\gamma\left[\frac{\partial N}{\partial y}\right]_{y=0}$ is the surface couple stress,

$Nu_x=\frac{xq_w}{k\left(T_w-T_0\right)}$ here $q_w=-k\left(\frac{\partial T}{\partial y}\right)_{y=0}$ be the surface heat flux and

$Sh_x = \dfrac{xq_m}{D_B\left(C_w - C_0\right)}$ here $q_m = -D_B\left(\dfrac{\partial C}{\partial y}\right)_{y=0}$ is the surface mass flux respectively. (13)

By use of Equation 7 in above Equation 13, we obtain their dimensionless form,

$$\left.\begin{aligned} &Cf_x\sqrt{\mathrm{Re}_x} = (1+K)\,f''(0),\\ &M_x\,\mathrm{Re}_x = \left(1+\frac{K}{2}\right)g'(0),\\ &Nu_x\left(\mathrm{Re}_x\right)^{-\frac{1}{2}} = -\theta'(0),\\ &Sh_x\left(\mathrm{Re}_x\right)^{-\frac{1}{2}} = -\phi'(0) \end{aligned}\right\} \quad (14)$$

where local Reynolds number denoted as $\mathrm{Re}_x = \dfrac{bx^2}{\nu}$.

3. Numerical Method

In this problem, 5th order Runge-Kutta-Fehlberg method with shooting technique is used to obtain numerical solution of ODE's system (Equation 8-11) along with the boundary conditions (Equation 12). Introduce the new set of variables

$$f = f_1,\ f' = f_2 = f_1',\ f'' = f_3 = f_2',\ g = f_4,\ g' = f_5 = f_4',\ \theta = f_6,\ \theta' = f_7 = f_6',\ \phi = f_8,\ \phi' = f_9 = f_8'$$

For conversion process of ODE, and we get the transformed algebraic equations are

$$f_1' = f_2,\ f_2' = f_3,\ f_3' = \left(\frac{1}{1+K}\right)\left\{f_2^2 - f_1 f_3 - Kf_5 - A^2 + \left(f_2 - A\right)\left(Ha + K^*\right)\right\},\ f_4' = f_5,$$

$$f_5' = \left(\frac{2}{2+K}\right)\left\{f_4 f_2 - f_1 f_5 + K\left(2f_4 + f_3\right)\right\},\ f_6' = f_7,\ f_7' = -\mathrm{Pr}\left(f_1 f_7 - f_2 f_6 - S_1 f_2 + Nbf_7 f_9 + Ntf_7^2\right),\ f_8' = f_9,$$

$$f_9' = \mathrm{Pr}\,Le\left\{\varepsilon f_8\left(1+f_6\delta\right)^m \exp\left(\frac{-E^*}{1+f_6\delta}\right) - f_1 f_9 + f_2 f_8 + S_2 f_2\right\} - \frac{Nt}{Nb}f_7'.$$

Along with the boundary conditions,

$$f_1 = 0,\ f_2 = 1,\ f_3 = m_1,\ f_4 = 0,\ f_5 = m_2,\ f_6 = 1 - S_1,\ f_7 = m_3,\ f_8 = 1 - S_2,\ f_9 = m_4 \text{ at } \eta = 0,$$

$$f_2 = A,\ f_4 = 0,\ f_6 = 0,\ f_8 = 0 \text{ as } \eta \to \infty.$$

Here, the boundary condition includes the unknown values m_1, m_2, m_3, m_4 for fixing η_∞ value. By changing distinct values of unknown values to satisfy $\eta \to \infty$ and do the same process until get two successive values of $f''(0), g'(0), \theta'(0)$ and $\phi'(0)$ (Senbagaraja and De [24]).

4. Results and Interpretation

During this session, we discovered the equivalence of the local skin friction coefficient and local couple stress of present result to previous references, the numerical tabulation of skin friction coefficient, local couple stress, local Nusselt number and local Sherwood number for notable values of separate parameters and the graphical visualization and analysis of various admissible parameters on velocity profile $f'(\eta)$, angular velocity profile $g(\eta)$, temperature profile $\theta(\eta)$ and concentration profile $\phi(\eta)$, which are replicated from Fig.2 to Fig.16.

Table 2 Reflects the comparison of local skin friction and local couple stress for various values of Hartmann number and micropolar constant at $\Pr = 0.71, Le = 0.28, Nb = 0.1$ and other parameters are taken as zero with existing results Eldabe et al. [4], he used Chebyshev finite difference method for calculations and Hsiao [3], he used accurate finite-difference method for numerical results compared with current study which is done by Runge-Kutta-Fehlberg 5th order method; shows the good concurrence with this current result.

Table 3 reveals that the increasing value of micropolar constant decays skin friction coefficient and enhances the local couple stress. The gain in porous parameter enrich both skin friction coefficient and local couple stress with fixed values of $A = 0.3, Ha = 0.2, \Pr = 6.2$. Skin friction refers the relation of shear stress on the fluid surface, it make resistance to the fluid flow. When the micropolar constant increase, the micro-rotation of fluid also increases, so fluid resistance may neglected, this decays the skin friction coefficient but porous medium block the free flow, enriching the skin friction. Local couple stress is denoted as resistance for rotational movement, here micropolar constant and porous parameter enrich the rotational resistance.

Table 4 shows that increment value of thermal stratification parameter and Prandtl number improves and decays the local Nusselt number respectively when they $\Pr = 6.2, S_1 = 0.1, Nb = 1, Nt = 0.5$ are fixed. The rate of heat transfer is known as local Nusselt number, stratification phenomena enrich it and Prandtl number is indirectly proportional to thermal diffusivity, so it decays the heat transfer rate. High value of porous parameter adds resistance to the fluid flow which thicker the thermal boundary layer and while heat absorbing process rich chemical reaction lowers the fluid temperature and decays the heat transfer rate.

Table 5 portrays the gradual improvement of chemical reaction rate and temperature ratio which boost the local Sherwood number and activation energy may decay the local Sherwood number with $m = 0.1, Le = 0.1, S_2 = 0.1, \Pr = 6.2, Nb = 1, Nt = 0.5$. Mass transfer rate is known as local Sherwood number, activation energy increase the fluid reactors movement, which affects the mass-conducting process of fluid flow. Strong chemical reaction enhances the mass diffusion near surface and increase mass transfer rate.

Figs.2-3 replicates the enhancement in both linear and angular velocity profile for increasing values of micropolar constant. Micropolar fluid has detailed microstructure property, like micro-inertia and micro rotational motion. When we increase micropolar nanofluids property, it will add some shear force to fluid flow and thinner micro rotation boundary layer, which will help to improve the velocity of nanoparticles in both linear and rotational fluid motion.

Fig.4 shows the mounting value of ratio of velocity boost the fluid velocity. The parameter A denotes the proportion of free stream and stretching velocities. Free stream velocity is directly proportional to ratio of velocity, so an increment in the parameter gives better fluid velocity.

Escalating values of Hartmann number decay the nanoparticle velocity shown in Fig.5. The dimensionless Hartmann number is relative to electromagnetic force, when it is high; it causes frictional action in fluid flow, which is lead to reduce the fluid velocity.

The velocity of fluid flow is down for growing values of the porous parameter as sketched in Fig.6. Porous structures add complexity to micropolar nanofluid flow because micropolar nanofluid has a micro-rotation nature when we create pores in the fluid flow medium which boosts the hydrodynamic resistance. By this phenomena, the velocity of fluid flow decays.

The Prandtl number defines the ratio between momentum diffusivity and thermal diffusivity. A higher Prandtl number creates more viscosity in fluid flow and it tends to lower thermal conductivity of nanoparticles in fluid. So acclivity in the Prandtl number diminishes the heat transfer of fluid marked in Fig.7.

An increment in thermal stratification parameter slows down the thermal conductivity property of fluid flow as sketched in Fig.8. Stratification means developing the different layers, when it comes to thermal stratification, it splits the fluid layer depending on the hottest to coldest one. This formation acts in micro-rotational fluid motion and can affect heat transfer in fluid flow.

The augmentation of Brownian motion parameter boosts the thermal conductivity of the fluid which shown in Fig.9. Random collisions on tiny particles known as Brownian motion, when they meet micropolar nanofluid act like effective mixer of particles, it improves the rotation motion and reduce the resistance of fluid flow. The result is favorable for heat transfer.

Fig.10. sketches the gain in Brownian motion parameter debilitates the concentration profile in fluid flow. The high molecular collisions improve the rotational motion of the micropolar fluid; this confused heavy flow affects the mass transfer of the fluid, so the concentration field may decrease.

Excellent heat transfer is derived when enrichment made in the thermophoresis parameter replicates in Fig.11. Suspended molecular dancing in the fluid flow due to temperature gradients means the thermophoresis effect, which can add extra energy to micropolar fluids and cause effective thermal conductivity by energetic particles.

A stronger Lewis number weakens the concentration profile shows in Fig.12. Lewis number is indirectly proportional to mass diffusivity, so enrichment in Lewis number make deceleration in mass transfer of fluid flow.

Fig.13 shows that enrichment of solutal stratification parameter weakens the concentration field in fluid flow. Fluctuation in the fluid layer with distinct concentrations of solutes is notated as solutal stratification and these fluctuated dissolved solutes have low mass transfer in the fluid. This concentration dependent layer formation makes concentration boundary layer as thinner and profile faster decays.

Fig.14 depicts the gain in chemical reaction rate decays the concentration profile. When chemical reactions happen in micropolar fluids, they have some consequences like slow diffusion in the fluid, so reactants face issues in motion. In endothermic reactions the chemical species is consumed and boundary layer becomes thin, which leads to decreases in concentration profile.

Ascending values of the fitted rate parameter give descending nature to concentration profile which portrays in Fig.15. When we fix a high fitted rate value, it collapses the concentration field and makes exponential term steeper, so the reaction term becomes stronger at high temperatures. Which shows aggressive solute consumption in surface and concentration become decays.

Increasing value of activation energy enrich the concentration profile which shown in Fig.16. In concentrated fluid flow, while increase the activation energy leads to low reaction rate and slow species consuming in fluid flow; that's why high concentration are retained in fluid flow which enrich the concentration.

5. Conclusions

This write-up analyses the thermal and solutal stratification in stagnant micropolar nanofluid flow embedded in porous medium with addition of chemical reaction and activation energy in stretched sheet. Different parameters are investigated with distinct values in pictorial representation session and also in numerical tabulation ways. Key findings are highlighted below:

- Comparison between both local skin friction coefficient and couple stress for different values of Hartmann number and micropolar constant with explored previous findings reveals good concurrence with the current result.
- Local skin friction coefficient enhances for porous parameter and decays for micropolar constant. Local couple stress improves for both porous parameter and micropolar constant.
- Gradual mounting values of thermal stratification parameter and Prandtl number arise and suppress the heat transfer rate, respectively. Porous parameter and chemical reaction rate constant are decays the heat transfer rate.
- Local Sherwood number gets boosted for increasing values of chemical reaction rate constant and temperature ratio and quite oppositely for activation energy.
- Acceleration in micro-polar constant have better enhancement in linear and rotational motion velocities.
- Ascending values of Hartmann number and porous parameter diminish the velocity of fluid and gain a straight opposite result for the ratio of velocity parameter.
- Temperature decomposes for high values of Prandtl number and thermal stratification parameters and develops for increasing numbers of Brownian motion parameter and thermophoresis parameter.
- Concentration field of fluid flow falls down for an acclivity in the Brownian motion parameter, Lewis number, solutal stratification parameter, chemical reaction rate constant and fitted rate parameter. This is enhanced for activation energy parameter.

6. Future Scope

* This study predominantly used in biomedical field due to micro-rotation fluid property and stagnation point flow, so we can extend this model for blood flow with various geometries.
* Adding specific nanoparticles to enhance the heat and mass transfer property of fluid such as hybrid fluid model.
* Performing entropy generation to reduce energy losses and for high efficiency result we can add sensitivity, stability analysis. Artificial neural network prediction also used to enhance the accuracy of results.

Nomenclature

a_1, a_2, d_1, d_2	Constants	N^*	Angular velocity of fluid (rad/s)
A	Ratio of stretching rate constant	Nb	Brownian motion parameter
b, e	Stretching rate constant (s^{-1})	Nt	Thermophoresis parameter
B	Magnetic field	Pr	Prandtl number
B_0	Intensity of magnetic field (A/m)	S_1	Thermal stratification parameter
C	Fluid's concentration (mol/m^3)	S_2	Solutal stratification parameter
C_0	Allusion concentration (mol/m^3)	T	Fluid's temperature (K)
C_w	Wall concentration (mol/m^3)	T_0	Allusion temperature (K)
C_∞	Atmosphere concentration (mol/m^3)	T_w	Wall temperature (K)
D_B	Brownian diffusion coeffeicent (m^2/s)	T_∞	Atmosphere temperature (K)
D_T	Thermophoresis diffusion coefficient (m^2/s)	U_w	Stretching velocity (m/s)
E_a	Activation energy (J)	U_e	Free stream velocity (m/s)
E^*	Activation energy parameter		**Greek symbol**
Ha	Hartmann number	α	Thermal diffusivity (m^2/s)
j	Micro inertia density (m^2)	δ	Temperature ratio
k_1	Permeability constant (m^2)	ε	Chemical reaction rate constant
k_f	Vortex viscosity ($Kg\ m^{-1}\ s^{-1}$)	γ	Spin gradient viscosity (N s)
K_r	Chemical reaction constant (s^{-1})	η	Similarity variable
K_1	Boltzmann constant (J/K)	μ	Dynamic viscosity (Pa s)
K	Micropolar constant	ρ	Fluid density (kg/m^3)
K^*	Porous parameter	σ	Electric strength of fluid (S/m)
Le	Lewis number	τ	Heat capacity ratio
m	Fitted rate	ν	Kinematic viscosity (m^2/s)

Author's contribution statement

Meena Rajeswari P: Conceptualization; Formal analysis; Investigation; Methodology; Validation; Writing-original draft; Writing-review and editing.

Poulomi De: Investigation; Methodology; Supervision; Validation; Writing-review and editing.

Funding: None

Conflicts of interest

The authors declare that they have no known competing financial interests or personal relationships that could have appeared to influence the work reported in this paper.

References

1. Eringen, E.C. "Theory of micropolar fluids", *J. Math. Mech.*, **16**, pp.1-18, (1966). DOI: https://www.jstor.org/stable/24901466
2. Eringen, E.C. "Theory of thermo-microfluids", *J. Math. Anal. Appl.*, **38**(2), pp.480-496, (1972). DOI: https://doi.org/10.1016/0022-247X(72)90106-0

3. Hsiao, K.L. "Micropolar nanofluid flow with MHD and viscous dissipation effects towards a stretching sheet with multimedia feature", *Int. J. Heat Mass Trans.*, **112**, pp.983-990, (2017). DOI: https://doi.org/10.1016/j.ijheatmasstransfer.2017.05.042
4. Eldabe, N.T. and Ouaf, M.E. "Chebyshev finite difference method for heat and mass transfer in a hydromagnetic flow of a micropolar fluid past a stretching surface with Ohmic heating and viscous dissipation", *Appl. Math. Comp.*, **177**(2), pp.561-71, (2006). DOI: https://doi.org/10.1016/j.amc.2005.07.071
5. Mishra, S.R., Khan, I., Mdallal, et al. "Free convective micropolar fluid flow and heat transfer over a shrinking sheet with heat source", *Case stud. Therm. Eng.*, **11**, pp.113-119, (2018). DOI: http://dx.doi.org/10.1016/j.csite.2018.01.005
6. Hsiao, K.L. "Stagnation electrical MHD nanofluid mixed convection with slip boundary on a stretching sheet". *Appl. Therm. Eng.*, **98,** pp.850-861, (2016). DOI: https://doi.org/10.1016/j.applthermaleng.2015.12.138
7. Soid, S.K., Ishak, A. and Pop, I. "MHD stagnation-point flow over a stretching/shrinking sheet in a micropolar fluid with a slip boundary", *Sains Malays.*, **47**(11), pp.2907-16, (2018). DOI: http://dx.doi.org/10.17576/jsm-2018-4711-34
8. Muhammad, S., Atif, M., Abbas, U., et al. "Stagnation point flow of EMHD micropolar nanofluid with mixed convection and slip boundary", *Complexity*, pp.1-13, (2021). DOI: https://doi.org/10.1155/2021/3754922
9. Hsiao, K.L. "Combined electrical MHD heat transfer thermal extrusion system using Maxwell fluid with radiative and viscous dissipation effects". *Appl. Therm. Eng.*, **112**, pp.1281-1288, (2017). DOI: https://doi.org/10.1016/j.applthermaleng.2016.08.208
10. Gamar, F., Shamshuddin, M.D., Ram, M.S., et al. "Exploration of thermal radiation and stagnation point in MHD micropolar nanofluid flow over a stretching sheet with Navier slip". *Numer. Heat Trans., A Appl.*, pp.1-13, (2024). DOI: https://doi.org/10.1080/10407782.2024.2338264
11. Atif, S.M., Hussain, S. and Sagheer, M. "Magnetohydrodynamic stratified bioconvective flow of micropolar nanofluid due to gyrotactic microorganisms", *Aip Adv.*, **9**(2), pp.1-16, (2019). DOI: https://doi.org/10.1063/1.5085742
12. Sarojamma, G., Lakshmi, R.V., Sreelakshmi, K. et al. "Dual stratification effects on double-diffusive convective heat and mass transfer of a sheet-driven micropolar fluid flow", *J. King Saud Univ., Sci.*, **32**(1), pp.366-76, (2020). DOI: https://doi.org/10.1016/j.jksus.2018.05.027
13. Alharbi, K.A., Khan, Z., Zuhra, S., et al. "Numerical study of the electromagnetohydrodynamic bioconvection flow of micropolar nanofluid through a stretching sheet with thermal radiation and stratification". *ACS Omega*, **7**(47), pp.42733-51, (2022). DOI: https://doi.org/10.1021/acsomega.2c04145
14. Farooq, M., Javed, M., Ijaz, K., et al. "Melting heat transfer and double stratification in stagnation flow of viscous nanofluid", *Res. Phys.*, **7**, pp.2296-2301, (2017). DOI: https://doi.org/10.1016/j.rinp.2017.06.053
15. Choudhary, S., Choudhary, P., Alessa, N. et al. "MHD Thermal and Solutal Stratified Stagnation Flow of Tangent Hyperbolic Fluid Induced by Stretching Cylinder with Dual Convection", *Mathematics*, **11**(9), pp.1-20, (2023). DOI: https://doi.org/10.3390/math11092182
16. Abbas Khan, A., Naveed Khan, M., Ahammad, N.A., et al. "Flow investigation of second grade micropolar nanofluid with porous medium over an exponentially stretching sheet". *J. Appl. Biomater. Funct. Mater.*, **20**, p.22808000221089782, (2022). DOI: https://doi.org/10.1177/22808000221089782

17. Mohanty, B., Mishra, S.R. and Pattanayak, H.B. "Numerical investigation on heat and mass transfer effect of micropolar fluid over a stretching sheet through porous media", *Alex. Eng. J.,* **54**(2), pp.223-232, (2015). DOI: https://doi.org/10.1016/j.aej.2015.03.010
18. Dadheech, A., Sharma, S. and Al-Mdallal, Q. "Numerical simulation for MHD Oldroyd-B fluid flow with melting and slip effect". *Sci. rep.*, **14**(1), p.10591, (2024). DOI: https://doi.org/10.1038/s41598-024-58376-1
19. Karthik, S., Iranian, D. and Al-Mdallal, Q.M. "Numerical simulation of magneto-hydrodynamic fluid flow with heat sink, chemical diffusion and Powell Eyring fluid behavior using Cattaneo–Christov source term". *Int. J. Thermofluids,* **22**, p.100616, (2024). DOI: https://doi.org/10.1016/j.ijft.2024.100616
20. De, P. "Bioconvection of nanofluid due to motile gyrotactic microorganism with ohmic heating effects saturated in porous medium", *BioNanoSci.*, **11**, pp.658-66, (2021). DOI: https://doi.org/10.1007/s12668-021-00844-3
21. Goyal, M., Tailor, M.V. and Yadav, R. "Stagnation point flow of MHD micropolar fluid in the presence of melting process and heat absorption/generation", *Generation Global Journal of Pure and Applied Mathematics,* **13**(9), pp.4889-907, (2017). DOI: https://www.ripublication.com/gjpam17/gjpamv13n9_37.pdf
22. Mishra, S.R., Nayak, B. and Sharma, R.P. "MHD stagnation-point flow past over a stretching sheet in the presence of non-Darcy porous medium and heat source/sink", *Defect Diffus. Forum,* **374**, pp.92-105, (2017). DOI: http://dx.doi.org/10.4028/www.scientific.net/DDF.374.92
23. Nisha, S.S. and De, P. "Impact of electro-osmotic, activation energy and chemical reaction on Sisko fluid over Darcy–Forchheimer porous stretching cylinder". *Proc. Inst. Mech. Eng. E J. Process Mech. Eng.*, p.09544089241255657, (2024). DOI: https://doi.org/10.1177/09544089241255657
24. Senbagaraja, P. and De, P. "Sensitivity analysis on electro-osmotic flow of EMHD tangent hyperbolic nanofluid through porous rotating disk with variable thermal conductivity, Stefan blowing and thermal radiation". *Multiscale Multidiscip. Model. Exp. Des.*, **8**(1), p.65, (2025). DOI: https://doi.org/10.1007/s41939-024-00648-4
25. Yesodha, P., Bhuvaneswari, B., Sivasankaran, S., et al. "Convective heat and mass transfer of chemically reacting fluids with activation energy with radiation and heat generation", *J. Therm. Eng.,* **7**(5), pp.1130-8, (2021). DOI: http://dx.doi.org/10.18186/thermal.977986
26. Prakash, D., Saraswathy, M. and Kumar, S. "Transient Convective Heating Transport of the Micropolar Fluid Flow Between Asymmetric Channel with Activation Energy", *IOP Conf. Ser.: Mater. Sci. Eng.*, **1130**, pp.012049, (2021). DOI: https://iopscience.iop.org/article/10.1088/1757-899X/1130/1/012049/pdf
27. Zeeshan, N.A., Ahammad, H.U., Rasheed, A.A., et al. "A numerical intuition of activation energy in transient micropolar nanofluid flow configured by an exponentially extended plat surface with thermal radiation effects", *Mathematics,* **10**(21), pp.4046, (2022). DOI: https://doi.org/10.3390/math10214046
28. Hsiao, K.L. "To promote radiation electrical MHD activation energy thermal extrusion manufacturing system efficiency by using Carreau-Nanofluid with parameters control method". *Energy*, **130**, pp.486-499, (2017). DOI: https://doi.org/10.1016/j.energy.2017.05.004
29. Lakshmi, D.G., Niranjan, H. and Sivasankaran, S. "Effects of chemical reactions, radiation, and activation energy on MHD buoyancy induced nanofluid flow past a vertical surface", *Sci. Iran.,* **29**(1), pp.90-100, (2022). DOI: https://doi.org/10.24200/sci.2021.56835.4934
30. Soliman, H.A. "Numerical Treatment of MHD Rotating Flow of Nano-Micropolar Fluid with Impact of Temperature-Dependent Heat Generation and Variable Porous Matrix", *MSA Eng. J.,* **1**(4), pp.98-112, (2022). DOI: https://doi.org/10.21608/msaeng.2022.277745

31. Vinodkumar Reddy, M., Lakshminarayana, P., Vajravelu, K. et al. "Activation of energy in MHD Casson nanofluid flow through a porous medium in the presence of convective boundary conditions and suction/injection", *Numer. Heat Transf. A: Appl.*, pp.1-17, (2023). DOI: https://doi.org/10.1080/10407782.2023.2271655
32. Raza, Q., Wang, X., Muhammed, H.A., et al. "Bio-convection of ternary magnetized nanoparticles thermal conductivity in chemical reaction and activation energy flow with Darcy Forchheimer permeable across a double porous medium", *Numer. Heat Transf. A: Appl.*, pp.1-26, (2024). DOI: https://doi.org/10.1080/10407782.2024.2316210
33. Gomari, S.R., Alizadeh, R., Alizadeh, A., et al. "Generation of entropy during forced convection of heat in nanofluid stagnation-point flows over a cylinder embedded in porous media", *Numer. Heat Transf. A: Appl.*, **75**(10), pp.647-73, (2019). DOI: https://doi.org/10.1080/10407782.2019.1608774
34. Vijayaragavan, R., Tamizharasi, P. and Magesh, A. "Peristaltic motion of non-Newtonian fluid under the influence of inclined magnetic field, porous medium and chemical reaction". *Sci. Iran.*, **31**(8), pp.632-645, (2024). DOI: https://doi.org/10.24200/sci.2024.59484.6270
35. Kalita, J.C. and Kumar, P. "Vortex dynamics of accelerated flow past a mounted wedge". *Phys. Fluids*, **35**(12), (2023). DOI: https://doi.org/10.1063/5.0177161
36. Kumar, P. and Kalita, J.C. "An efficient ψ-v scheme for two-dimensional laminar flow past bluff bodies on compact nonuniform grids". *Int. J. Numer. Meth. Fluids*, **92**(12), pp.1723-1752, (2020). DOI: https://doi.org/10.1002/fld.4846
37. Kumar, P. and Kalita, J.C. "A transformation-free ψ-v formulation of the Navier–Stokes equations on compact nonuniform grids". *J. C. Appl. Math.*, **353**, pp.292-317, (2019). DOI: https://doi.org/10.1016/j.cam.2018.12.035
38. Khan, A., Rajendran, P., Sidhu, J.S.S., et al. "Convolutional neural network modeling and response surface analysis of compressible flow at sonic and supersonic Mach numbers". *Alex. Eng. J.*, **65**, pp.997-1029, (2023). DOI: https://doi.org/10.1016/j.aej.2022.10.006

List of Figure Caption:

Figure.1. Flow Configuration and Coordinate System

Figure.2: Micro polar constant molded on velocity profile

Figure.3: Micro polar constant molded on angular velocity profile

Figure.4: Ratio of velocities molded on velocity profile

Figure.5: Hartmann number molded on velocity profile

Figure.6: Porous parameter molded on velocity profile

Figure.7: Prandtl number molded on temperature profile

Figure.8: Thermal stratification parameter molded on temperature profile

Figure.9: Brownian motion parameter molded on temperature profile

Figure.10: Brownian motion parameter molded on concentration profile

Figure.11: Thermophoresis parameter molded on temperature profile

Figure.12: Lewis number parameter molded on concentration profile

Figure.13: Solutal stratification parameter molded on concentration profile

Figure.14: Chemical reaction rate constant molded on concentration profile

Figure.15: Fitted rate parameter molded on concentration profile

Figure.16: Activation energy parameter molded on concentration profile

List of Table Caption:

Table 1: Brief Inspection of Literatures to Pinpoint Research Gaps

Table 2: Comparison of local skin friction coefficient $(-f''(0))$ and local couple stress $(g'(0))$ for distinguishable Hartmann number (Ha) and porous parameter (K)

Table 3: Numerical tabulation for skin friction coefficient and local couple stress of micropolar constant (K) and porous parameter (K^*)

Table 4: Numerical tabulation of local Nusselt number $(-\theta'(0))$ for thermal stratification parameter (S_1), Prandtl number (Pr), porous parameter (K^*) and chemical reaction (ε)

Table 5: Numerical tabulation of local Sherwood number $(-\phi'(0))$ for chemical reaction rate (ε), activation energy (E^*) and temperature ratio (δ)

Keywords / Author	Micropolar Nanofluid	Stagnation Point	Stratification	Porous Medium	Activation Energy	Chemical Reaction
Hsiao [3]	✓	×	×	×	×	×
Gamar et al. [10]	✓ (Micropolar fluid)	✓	×	×	×	×
Alharbi et al. [13]	✓	×	✓	×	×	✓
Nisha and De [23]	×	×	×	✓	✓	✓
Vijayaragavan et al. [34]	×	×	×	✓	×	✓
Current Study	✓	✓	✓	✓	✓	✓

Table 1: Brief Inspection of Literatures to Pinpoint Research Gaps

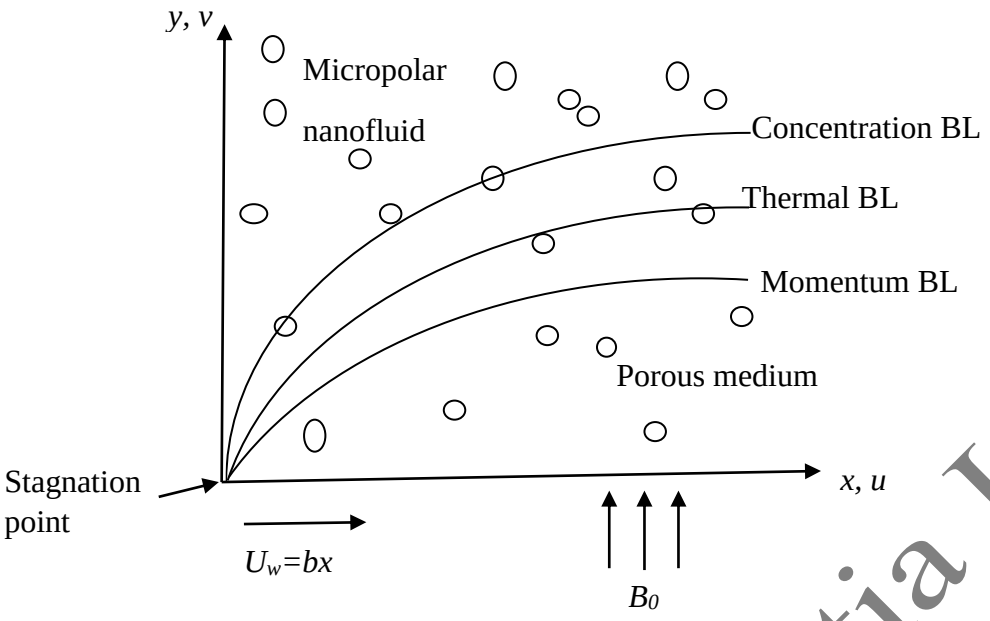

Figure.1. Flow Configuration and Coordinate System

Ha	*K*	**Eldabe and Ouaf [4]** $-f''(0)$	**Hsiao [3]** $-f''(0)$	**Current result** $-f''(0)$	**Eldabe and Ouaf [4]** $g'(0)$	**Hsiao [3]** $g'(0)$	**Current result** $g'(0)$
		Chebyshev finite difference method	Accurate finite difference method	RKF 5th order method	Chebyshev finite difference method	Accurate finite difference method	RKF 5th order method
0.0	0.2	0.9098	0.9098	0.9097	0.0950	0.0950	0.0950
0.5	0.2	1.1148	1.1147	1.1144	0.1051	0.1051	0.1050
1.0	0.2	1.2871	1.2871	1.2871	0.1121	0.1121	0.1121
1.0	0.0	1.4142	1.4142	1.4142	0	0	0
1.0	0.5	1.1407	1.1408	1.1407	0.2112	0.2112	0.2111
1.0	2.0	0.7696	0.7697	0.7696	0.3586	0.3586	0.3585

Table 2: Comparison of local skin friction coefficient ($-f''(0)$) and local couple stress ($g'(0)$) for distinguishable Hartmann number (Ha) and porous parameter (K)

K	K^*	**skin friction coefficient**	**local couple stress**
0.1	2.0	1.2759	0.0452
0.2		1.2200	0.0827
0.3		1.1700	0.1144
0.1	2.2	1.3103	0.0455
	2.4	1.3437	0.0459

Table 3: Numerical tabulation for skin friction coefficient and local couple stress of micropolar constant (K) and porous parameter (K^*)

S_1	Pr	K^*	ε	$-\theta'(0)$
0.1	6.0	1.0	0.1	0.9407
	6.1			0.9365
	6.2			0.9322
0.2				0.9430
0.3				0.9538
0.1		2.0	0.2	0.9817
		3.0		0.9808
		4.0		0.9785
			2.2	0.9597
			4.2	0.9419

Table 4: Numerical tabulation of local Nusselt number ($-\theta'(0)$) for thermal stratification parameter (S_1), Prandtl number (Pr), porous parameter (K^*) and chemical reaction (ε)

ε	E^*	δ	$-\phi'(0)$
0.1	0.1	0.1	0.5271
0.3			0.6227
0.5			0.7087
0.1	0.3		0.5182
	0.5		0.5108
	0.1	0.3	0.5278
		0.5	0.5284

Table 5: Numerical tabulation of local Sherwood number ($-\phi'(0)$) for chemical reaction rate (ε), activation energy (E^*) and temperature ratio (δ)

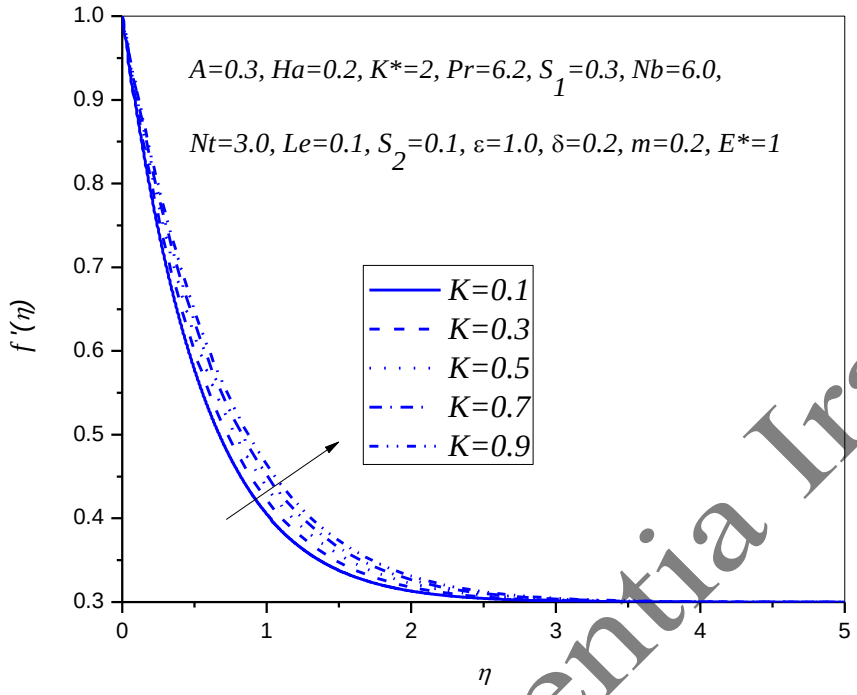

Figure.2 Micro polar constant molded on velocity profile

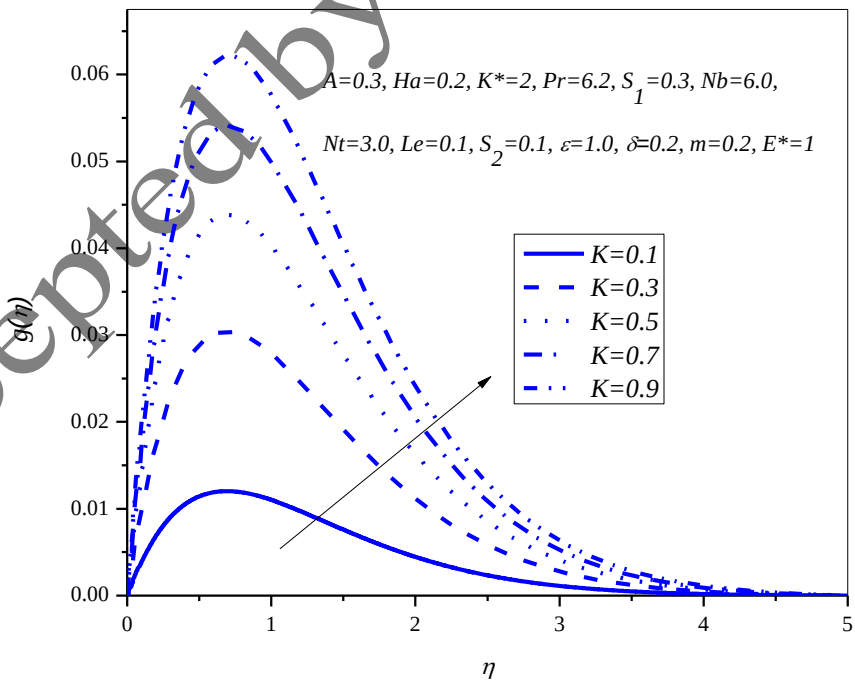

Figure.3 Micro polar constant molded on angular velocity profile

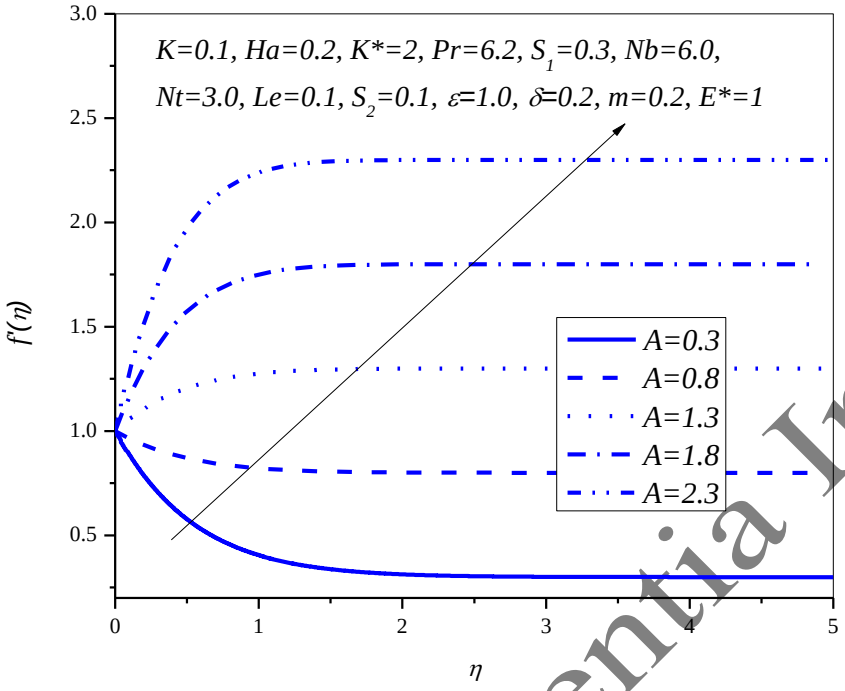

Figure.4 Ratio of velocities molded on velocity profile

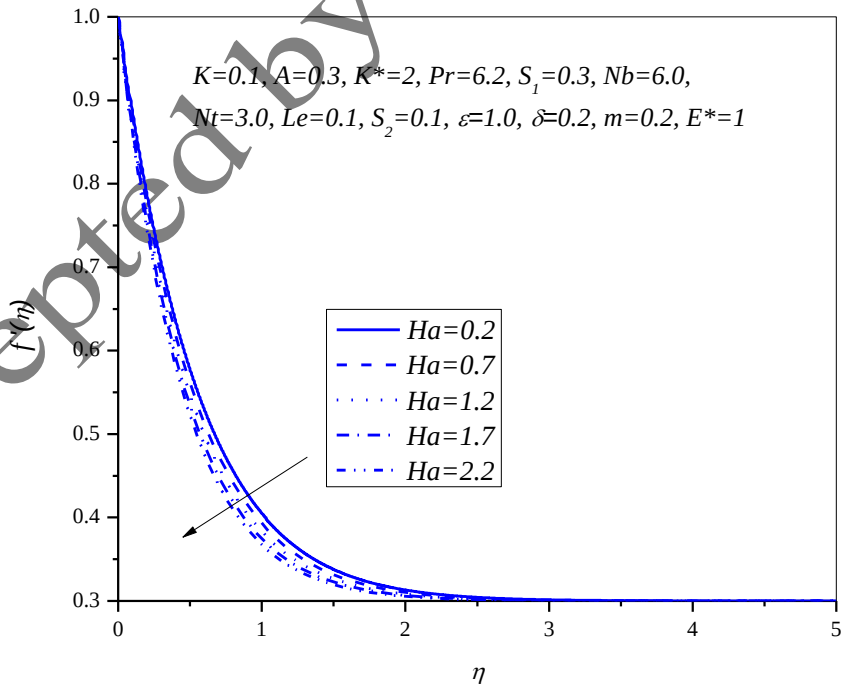

Figure.5 Hartmann number molded on velocity profile

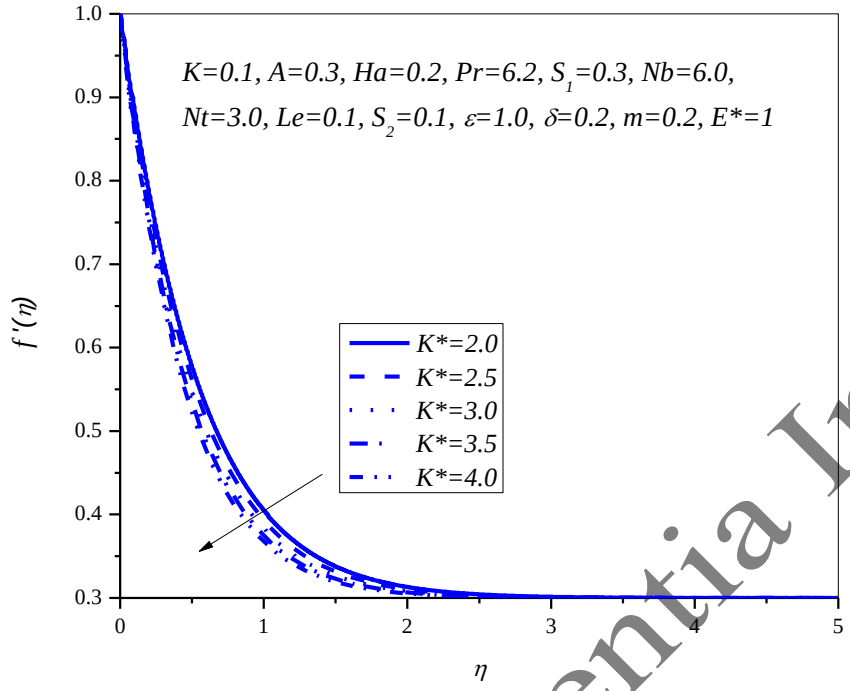

Figure.6 Porous parameter molded on velocity profile

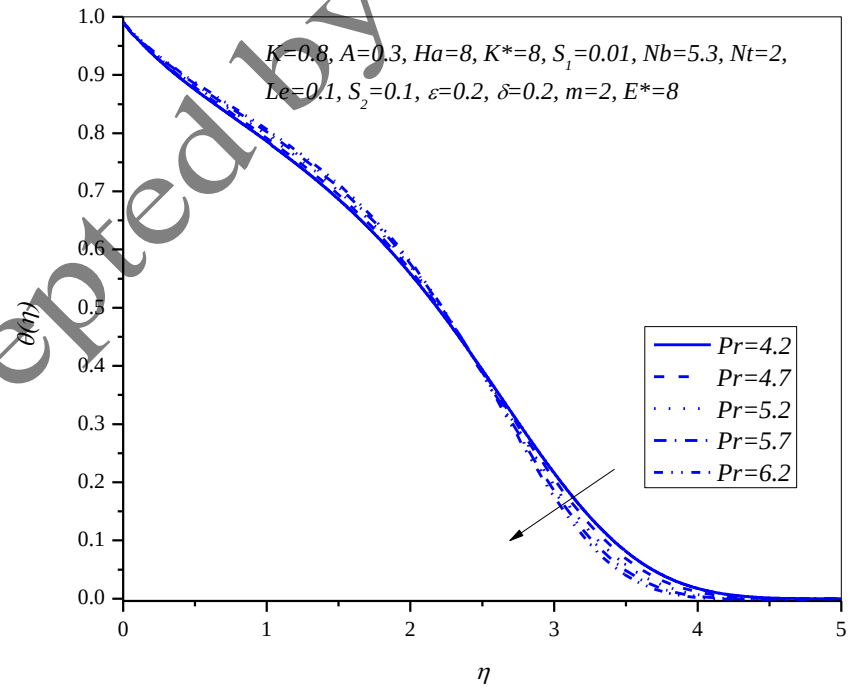

Figure.7 Prandtl number molded on temperature profile

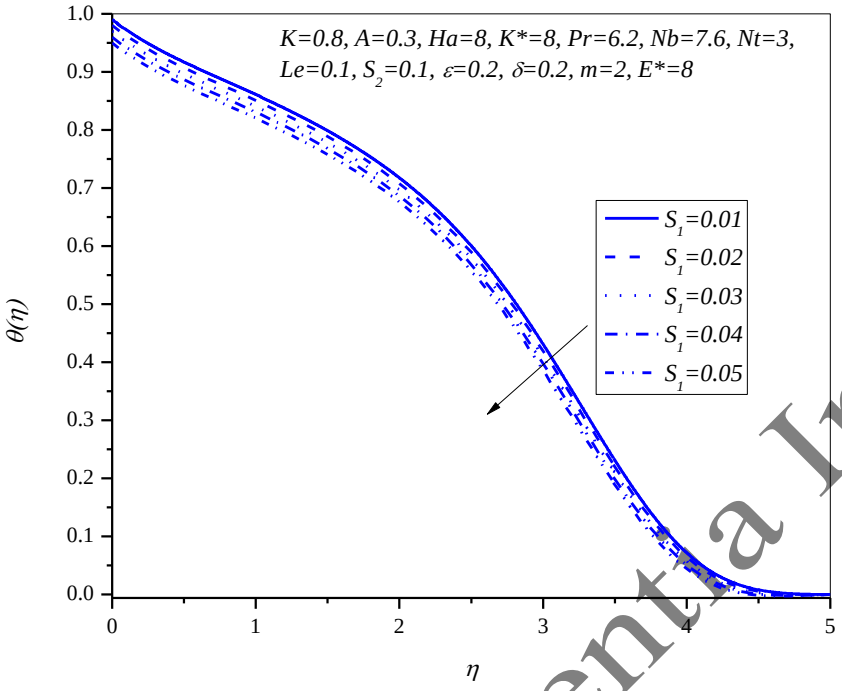

Figure.8 Thermal stratification parameter molded on temperature profile

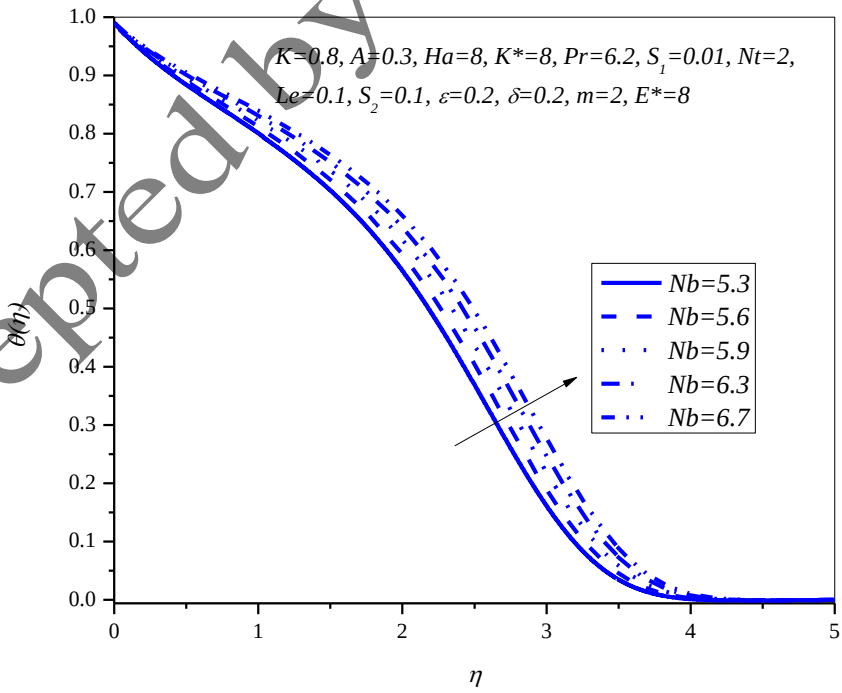

Figure.9 Brownian motion parameter molded on temperature profile

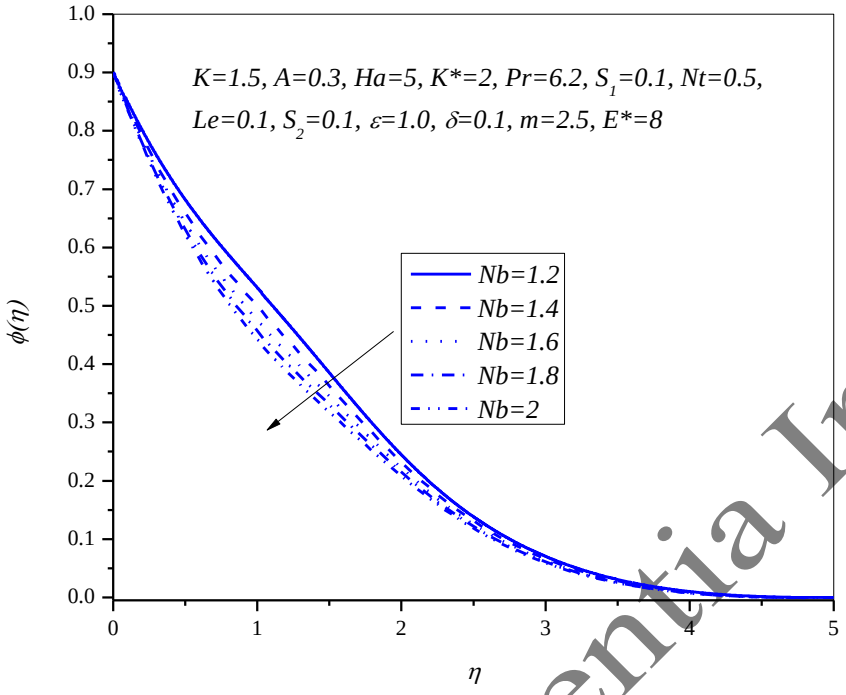

Figure.10 Brownian motion parameter molded on concentration profile

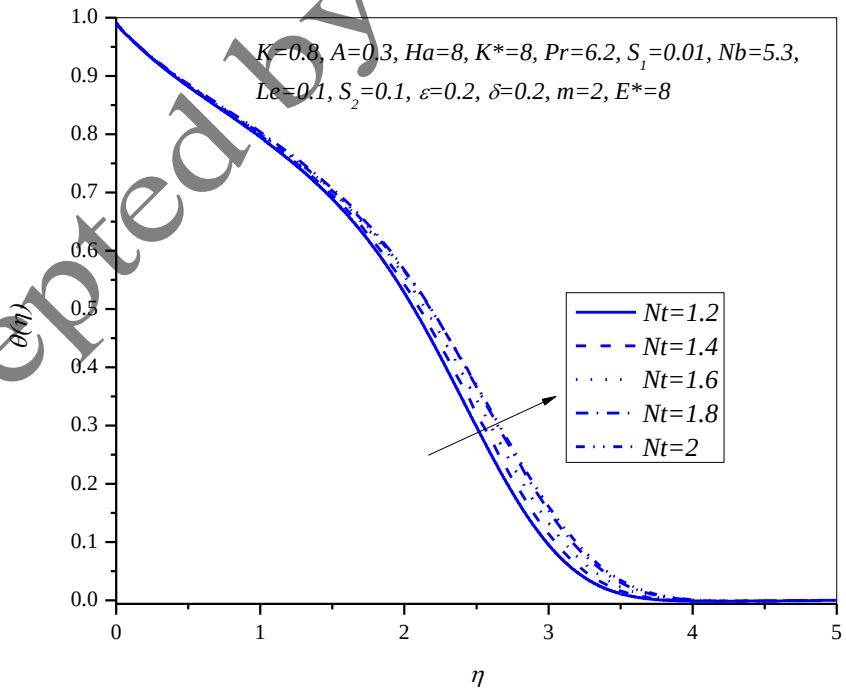

Figure.11 Thermophoresis parameter molded on temperature profile

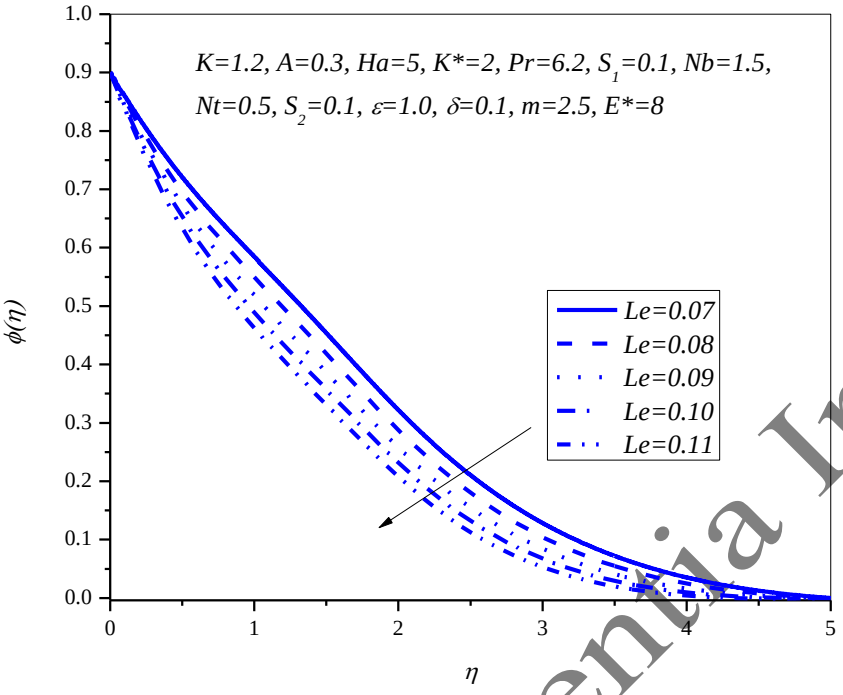

Figure.12 Lewis number parameter molded on concentration profile

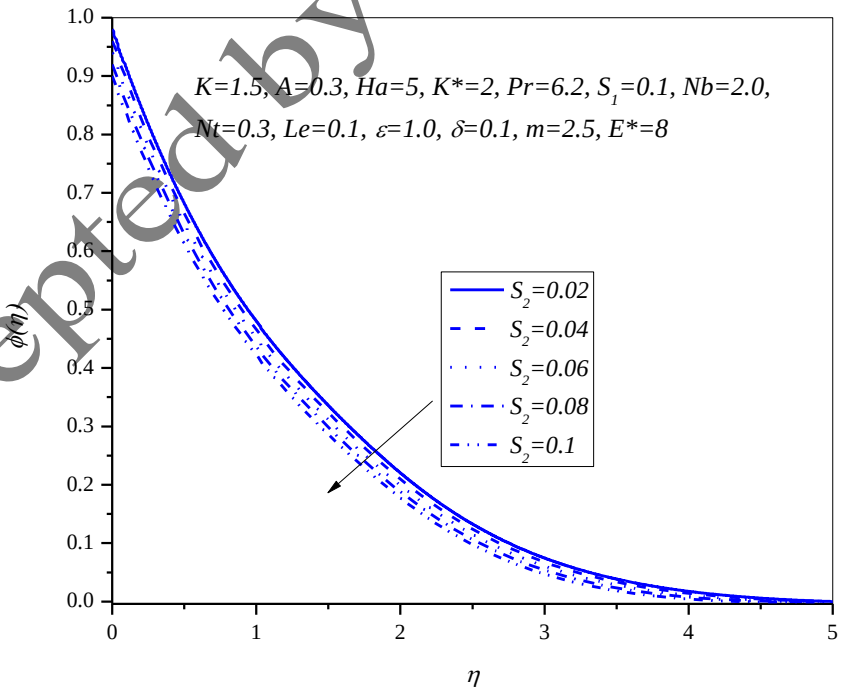

Figure.13 Solutal stratification parameter molded on concentration profile

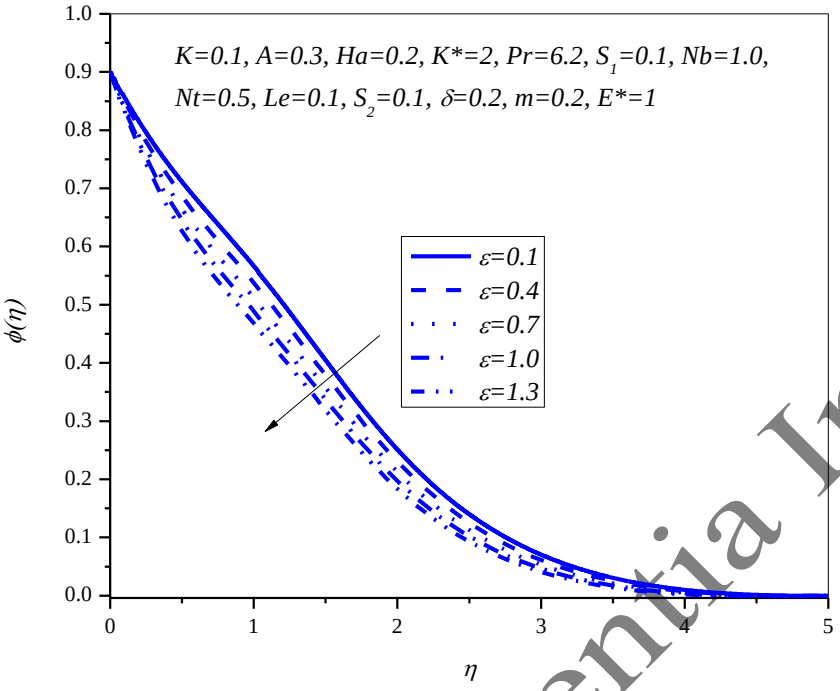

Figure.14 Chemical reaction rate constant molded on concentration profile

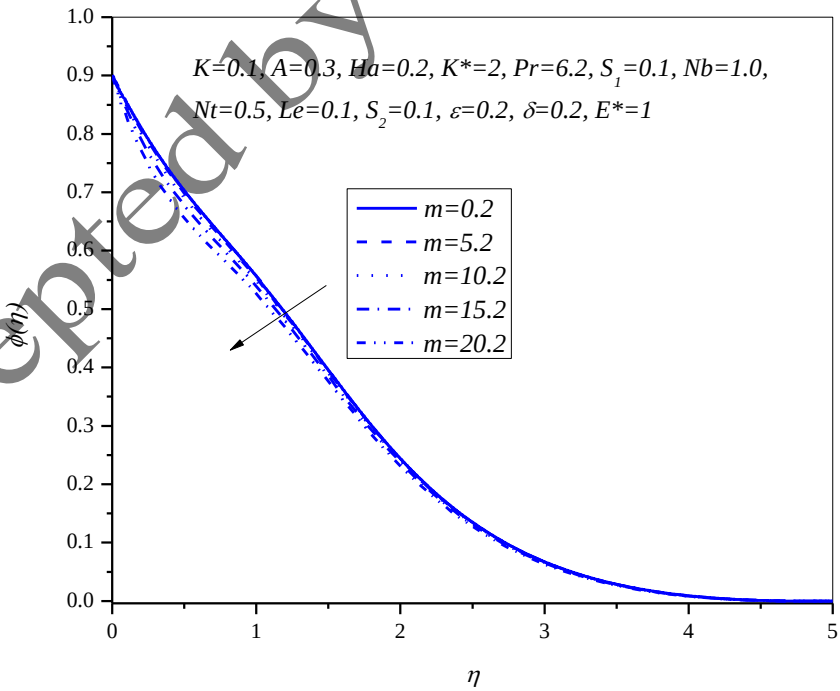

Figure.15 Fitted rate parameter molded on concentration profile

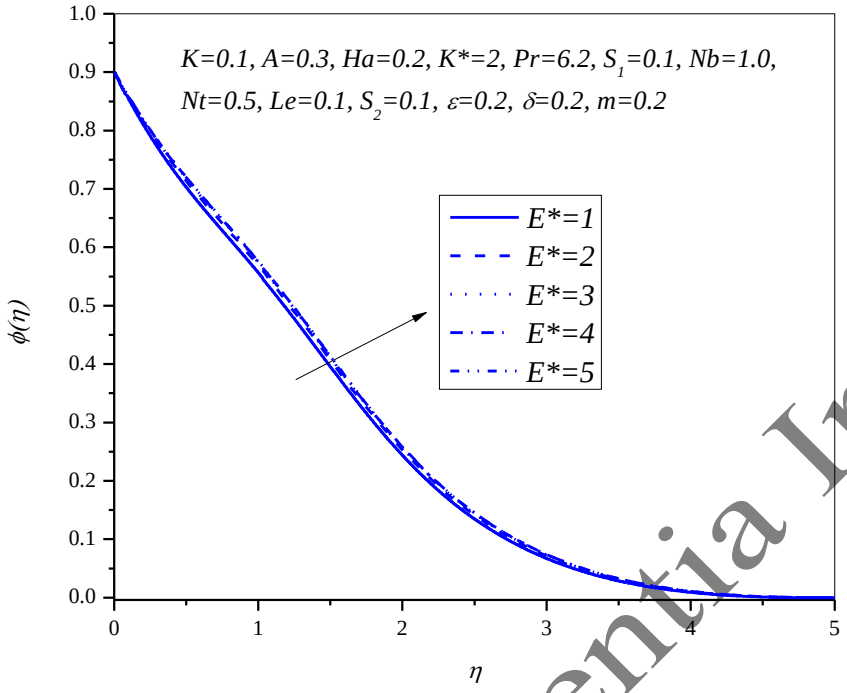

Figure.16 Activation energy parameter molded on concentration profile

Biographies

P. Meena Rajeswari was born in Tamilnadu, India, in 1999. She is currently pursuing her Ph.D. program in the field of fluid dynamics at Vellore Institute of Technology (VIT), Chennai, Tamilnadu, India. She completed her M.Sc. in the year of 2022 from The American College, Madurai, Tamilnadu, India. Her current research focuses on fluid dynamics, blood flow analysis and Hybrid nanofluid flow.

Poulomi De received her PhD degree in May, 2016 from National Institute of Technology, Agartala, India and published more than 40 papers in various reputed journals. She has been working as Assistant Professor Senior Grade 1 at Vellore Institute of Technology, Chennai, India since 2017. Her current research includes hybrid nanofluids, non- Newtonian fluids, bioconvection phenomenon etc.